DOI: 10.1002/anie.201003870

Photovoltaics

Flexible, Light-Weight, Ultrastrong, and Semiconductive Carbon Nanotube Fibers for a Highly Efficient Solar Cell**

Tao Chen, Shutao Wang, Zhibin Yang, Quanyou Feng, Xuemei Sun, Li Li, Zhong-Sheng Wang, and Huisheng Peng**

Carbon nanotubes have been widely introduced to fabricate high-efficiency organic solar cells because of their extremely high surface area (e.g., ca. 1600 $m^2 g^{-1}$ for single-walled nanotubes[1]) and superior electrical properties.[2] In one direction, nanotubes are used in electrode materials. For example, the incorporation of nanotubes onto titania nanoparticle films has been shown to increase the roughness factor and decrease the charge recombination of electron/hole pairs,[3,4] and the replacement of platinum with nanotubes as counter electrode catalyzed the reduction of triiodide to improve the cell performance.[5] In another direction, the distribution of nanotubes within the photoactive layer improved the short circuit current density and fill factor owing to rapid charge separation at the nanotube/electron donor interface and efficient electron transport through nanotubes.[6,7] However, the degrees of improvement are far from what is expected for nanotubes, mainly because of random aggregation of nanotubes in the cells.[8] For a random nanotube network, the electrons have to cross many more boundaries.[9] Therefore, alignment of nanotubes will further greatly improve cell performance as charge transport is more efficient.

[*] T. Chen,[+] S. Wang,[+] Z. Yang, Q. Feng, X. Sun, Dr. L. Li, Prof. Z.-S. Wang, Prof. H. Peng
Laboratory of Advanced Materials, Fudan University
Shanghai 200438 (China)
E-mail: zs.wang@fudan.edu.cn
penghs@fudan.edu.cn
T. Chen,[+] Z. Yang, X. Sun, Dr. L. Li, Prof. H. Peng
Key Laboratory of Molecular Engineering of Polymers of Ministry of Education, Fudan University (China)
T. Chen,[+] Z. Yang, X. Sun, Dr. L. Li, Prof. H. Peng
Department of Macromolecular Science, Fudan University (China)
S. Wang,[+] Prof. Z.-S. Wang
Department of Chemistry, Fudan University (China)
[+] These authors contributed equally to this work.

[**] We thank Dr. Q. Shen at SIMIT for the catalyst support. This work was sponsored by the Natural National Science Foundation of China (20904006, 20971025, 90922004), National Basic Research Program of China (2011CB933302, 2011CB932503), Science and Technology Commission of Shanghai Municipality (1052nm01600, 09J1401100, 090J1401300, 10530705300), Shanghai Leading Academic discipline Project (B108), Jiangsu Major IAR Program (BY2010147), Program for New Century Excellent Talents in University (NCET-09-0318), and Scientific Research Foundation for the Returned Overseas Chinese Scholars, Ministry of Education of China, and Program for Key Discipline Creativity Talents at Fudan University.

Supporting information for this article is available on the WWW under http://dx.doi.org/10.1002/anie.201003870.

Solar cells have typically been fabricated from rigid plates, which are unfavorable for many applications, especially in the fields of portable and highly integrated equipment.[10,11] As a result, flexible devices have recently become the subject of active research as a good solution.[10] In particular, weavable fiber solar cells are very promising and have attracted increasing attention in recent years. Fiber solar cells based on metal wires, glass fibers, or polymer fibers have been investigated.[12–17]

Herein, we first made a family of novel organic solar cells with excellent performance from the highly aligned nanotube fiber. Compared with traditional solar cells fabricated from rigid plates or recently explored flexible films/fibers, nanotube fiber solar cells demonstrate some unique and promising advantages. Firstly, as the building nanotubes are highly aligned, the fiber shows excellent electrical properties,[18–24] which provide the novel solar cell with higher short-circuit photocurrent, better maximum incident monochromatic photon-to-electron conversion efficiency, and higher power conversion efficiency. Secondly, nanotube fibers show excellent mechanical properties, much stronger than Kevlar and comparable to the strongest commercial fibers of zylon and dyneema in tensile strength.[18] Thirdly, these fibers are flexible, light-weight, and weavable and have tunable diameters ranging from micrometers to millimeters.[21] The above properties provide nanotube fiber solar cells with a broad spectrum of applications, including power regeneration for space aircraft and clothing-integrated photovoltaics.

To produce desired nanotube fibers, high-quality nanotube arrays were first synthesized by a typical chemical vapor deposition method. The synthetic details are reported elsewhere.[23] To summarize, Fe/Al_2O_3 was used as the catalyst, ethylene served as the carbon source, and Ar with 6% H_2 was used to carry the precursor to a tube furnace, where the growth took place. The reaction temperature was controlled at 750 °C and the reaction time was typically between 10 and 20 min. Fibers were directly spun from the nanotube array (see Figure S1 in the Supporting Information), and the fiber diameter was controlled from 6 to 20 μm by varying the initial ribbon, that is, a bunch of nanotubes pulled out of the array at the beginning of the spinning. The nanotube fiber can be spun with lengths of tens of meters or even longer, and the fiber is uniform in diameter. The density of the nanotube fiber was calculated to be on the order of 1 $g cm^{-3}$, and its linear density was on the order of 10 $\mu g m^{-1}$, relative to 10 $mg m^{-1}$ and 20–100 $mg m^{-1}$ for cotton and wool yarns, respectively.[19] As shown in Figure 1 a, the nanotube fiber is flexible and will not break after being bent, folded, or even tied many times. High-resolution transmission electron microscopy (see Figure 1 b)

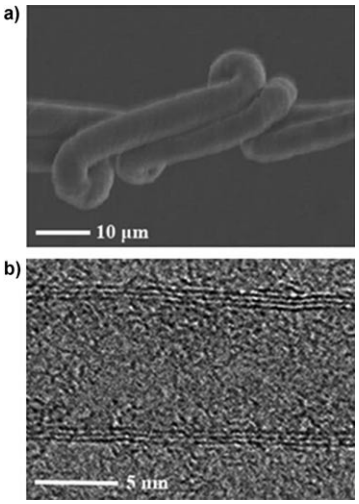

Figure 1. Carbon nanotube fibers characterized by scanning electron microscopy (SEM) and transmission electron microscopy (TEM). a) Knots could be tied in the nanotube fibers, revealing its high flexibility and resistance to torsion. b) High-resolution TEM image of a component nanotube.

indicates a multiwalled structure for the building nanotubes with diameter of approximately 8.5 nm in the fiber.

The high degree of alignment of the component nanotubes gives the fiber excellent mechanical and electrical properties. As shown in Figure 2a, the nanotube fiber demonstrates much higher values in both specific strength and specific stiffness than current engineering fibers. For example, the specific strength of a nanotube fiber is 2.9 times that of T1000, the strongest commercial fiber, and the specific stiffness is 3.9 times that of M70J, the stiffest commercial fiber. The electrical conductivity of the nanotube fiber ranges from 10^2 to 10^3 S cm^{-1} at room temperature. Figure 2b shows the temperature dependence of the conductivity of a fiber between 5 and 310 K measured by a four-probe method. The conductivities increase with increasing temperatures, suggesting semiconducting behavior.[23,24] The semiconducting properties of nanotube fibers may be very important to their optoelectronic applications. For example, these nanotube fibers can be used to replace titanium dioxide nanoparticles to fabricate high-performance dye-sensitized solar cells. The electron transport could be much faster along nanotubes than nanoparticles with abundant grain boundaries, and the charge separation of electrons and holes would be more efficient.[9] In addition, the work functions of nanotubes could be further tuned to match the used dyes in devices by surface modifications such as oxidative treatments through the use of air, oxygen plasma, or acid.[25] This treatment will further improve the electron transport between dye molecules and nanotubes. Further analysis (see Figure S2 in the Supporting Information) indicates that conduction in the fiber is mainly controlled by a three-dimensional hopping mechanism, and the calculation details are reported elsewhere.[23] Electrons could not be confined along the fiber and may hop from one site to another in a nanotube, or possibly from one nanotube to another. The three-dimensional conduction in the nanotube fiber is critical to the high performance of the derived solar cell, which will be detailed later.

The nanotube fiber shows a high surface area typically on the order of 10^2 m^2 g^{-1}.[26] Therefore, a wide variety of materials, including inorganic moieties such as gold nanoparticles,[2] small organic molecules,[24] polymers,[24] and hybrid inorganic/organic molecules such as γ-isocyanatopropyltriethoxysilane, could be easily physically incorporated or chemically bonded onto nanotubes in a fiber.[23] The confocal laser scanning microscopy image in Figure 3a shows a nanotube fiber after incorporation of 10,12-pentacosadiynoic acid followed by photopolymerization. The red color corresponds

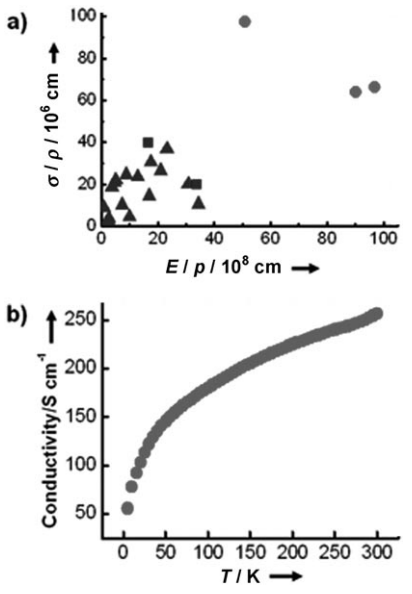

Figure 2. Mechanical and electrical properties of nanotube fibers. a) Mechanical properties of nanotube fibers (●) compared with other fiber materials such as engineering fibers (▲) and carbon fibers (■). The symbols σ, E, and ρ represent tensile stress, Young's modulus, and density, respectively. σ/ρ is the specific strength, E/ρ is the specific stiffness. b) Temperature dependence of the conductivity for a nanotube fiber.

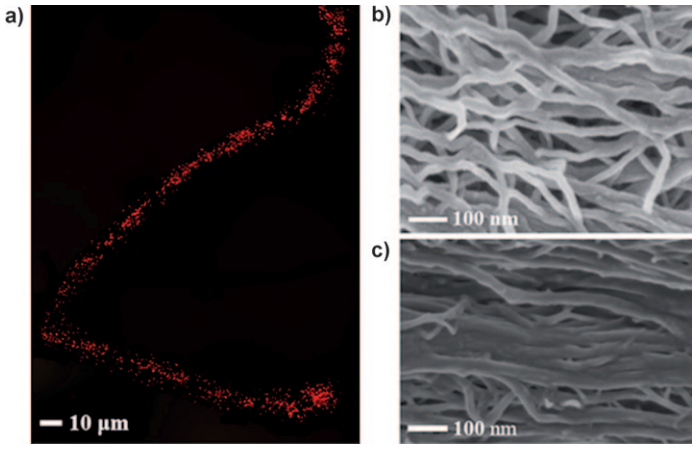

Figure 3. Incorporation of organic components into nanotube fibers. a) Confocal laser scanning microscopy image of a nanotube fiber after incorporation of diacetylene followed by photopolymerization. b,c) SEM images of a nanotube fiber before (b) and after (c) incorporation of N719.

to the derived fluorescent polydiacetylene, which is well distributed in the nanotube fiber. Figure 3 b,c compares SEM images inside a nanotube fiber before and after incorporation of the dye molecule bis(tetrabutylammonium) *cis*-diisothiocyanato-bis(2,2′-bipyridyl-4,4′-dicarboxylato)ruthenium(II) (also called N719; chemical structure shown in Figure S3 in the Supporting Information). N719 molecules were also well distributed among nanotubes in the fiber.

N719 was mainly loaded on the outer surfaces of building nanotubes through π–π interactions and van der Waals forces. The interactions between N719 molecules and nanotubes were confirmed by Raman spectra (Figure S4).[27,28] The characteristic peak of the NCS group shifted from 2104 cm^{-1} for pure N719 to 2098 cm^{-1} for N719/nanotube composite fibers, and the bipyridine vibration at 1540 cm^{-1} for pure N719 shifted to 1534 cm^{-1} for N719/nanotube composites;[27] both D-band and G-band peaks at 1344 and 1576 cm^{-1} for pure nanotubes shifted to 1347 and 1580 cm^{-1} for N719/nanotube composite fibers, respectively,[28] and the intensity ratios between G-band and D-band peaks decreased from 1.69 for pure nanotube fibers to 1.55 for N719/nanotube composite fibers. Note that for a pure nanotube fiber, the G band is much stronger than that of the D band, which indicated that the building nanotubes were very clean with less amorphous carbon or other impurities (also confirmed by Figure 1 b).

We used nanotube/N719 composite fibers to fabricate the organic solar cells on fluorine-doped tin oxide (FTO), and the experimental details are described in the Supporting Information. The above cells were tested under simulated AM 1.5 G illumination (100 mW cm^{-2}). The power conversion efficiencies ranged from 2.1 to 2.6 %. The current density/voltage (*J*–*V*) characteristics and the corresponding parameters of a typical device are further shown in Figure 4 a. Impressively, a solar cell fabricated with a composite fiber (5 mm long and 6 μm in diameter) produced a short-circuit photocurrent (J_{sc}) of 10.3 mA cm^{-2}, open-circuit photovoltage (V_{oc}) of 0.47 V, and fill factor (FF) of 0.45. The power conversion efficiency (η) can be then calculated to be 2.2 %. It should be noted that although the N719-adsorbed conductive glass can also produce photocurrent, the J_{sc} value (0.008–0.03 mA cm^{-2}) is negligible relative to that of the device, and pure nanotube fiber could not produce photocurrent under the same illumination. Therefore, the N719-loaded composite fiber rather than the pure nanotube fiber or the N719 alone is responsible for the observed photocurrent.

To further confirm the obtained J_{sc} value, the incident photon-to-electron conversion efficiency (IPCE) as a function of wavelength was measured and compared with the UV/Vis absorption spectrum of the N719 in solution (Figure 4 b). The two spectra are very similar, which indicates that N719 is the source of photocurrent generation. The photocurrent obtained by integrating the action spectrum with the standard AM 1.5 G solar emission spectrum is calculated to be 10.1 mA cm^{-2}, which is consistent with that under the simulated solar illumination (100 mW cm^{-2}). In addition, the IPCE value at 530 nm (an absorption peak for N719) is higher than 90 % and approaches 100 % if the absorption and reflection of the electrode are taken into account.[29] Thus, high light-harvesting efficiency, electron injection, and charge collection are achieved simultaneously.

Observation of anodic photocurrent generated from the nanotube/N719 composite (Figure S5) indicates that photocurrent is generated by electron injection from excited N719 molecules into the conduction band of nanotubes followed by transportation along the nanotubes, collection by the charge collector, and flow through external circuit to the counter electrode. The resulting dye cations are reduced to neutral state by I^- ions with production of I_3^- ions. I_3^- reverts to I^- by accepting electrons at the counter electrode. No net chemical reaction occurs after the completeness of a circuit, and photocurrent is continuously produced by regeneration of N719 and redox couples. The production and transportation of photoelectrons in the nanotube fiber are shown schematically in Figure 4 c. The photovoltage comes from the energy difference between the Fermi level of the semiconducting nanotubes and the electrochemical potential of the redox

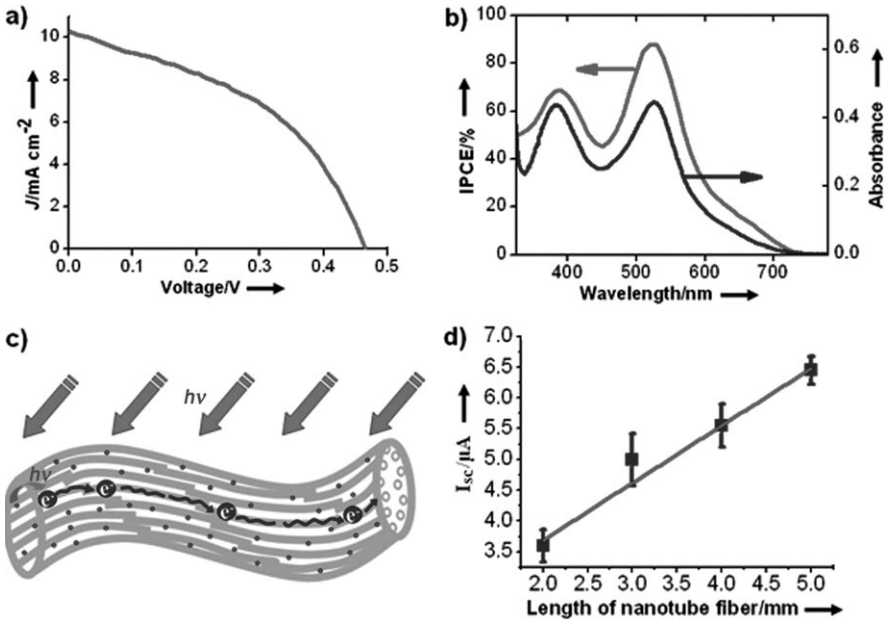

Figure 4. Characterizations of nanotube fiber solar cells. a) *J*–*V* curve of a solar cell under simulated 100 mW cm^{-2} illumination. J_{sc} = 10.3 mA cm^{-2}, V_{oc} = 0.47 V, FF = 0.45, η = 2.2 %. b) IPCE action spectrum (upper line) of the device and the UV/Vis absorption spectrum of N719 in ethanol (lower line). c) Diagram of the production and transportation of photoelectrons in a nanotube/N719 composite fiber. The top arrows represent sunlight. The tube, dots, and spheres correspond to the nanotube, N719, and photoelectrons, respectively. d) Dependence of the short-circuit current on the length of nanotube fibers in solar cells.

couple in the electrolyte. As the aligned nanotubes exhibit a three-dimensional conduction model, the transportation of electrons among them is very effective. According to the above working process, it is easy to understand that the photocurrent linearly increases with the increasing length of the fiber solar cell (Figure 4d).

To better understand the above mechanism, we compared the power conversion efficiencies of solar cells fabricated from nanotube fibers before and after treatment with strong nitric acid. The acidic treatment can produce carboxy groups on the surfaces of building nanotubes, and the modification may vary the Fermi levels of nanotubes.[30] Figure S6 compares the Raman spectra of a nanotube fiber before and after acidic treatment. After acidic treatment, the G-band peak largely decreases in intensity and shifts to shorter wavelength, while the D-band peak increases in intensity and shifts to longer wavelength. As expected, the solar cell showed a decrease of photocurrent from 6.1 to 4.1 μA, and the power conversion efficiency decreased from 2.2 to 1.5%. However, it was found that the increasing density of nanotubes in the fiber solar cell greatly improved the transportation efficiency of photoelectrons. For example, a nanotube fiber shrank 20% in diameter after solvent treatment, and the resulting solar cell showed a power conversion efficiency of around 4.0% compared to 2.2% before treatment. We also made nanotube-fiber organic solar cells on flexible substrate of ITO–PEN (ITO = indium tin oxide; PEN = polyethylene naphthalate) rather than FTO through a similar fabrication process. The resulting flexible devices exhibited power conversion efficiencies close to those on FTO. Typically, the efficiency ratio $\eta_{ITO-PEN}/\eta_{FTO}$ was around 0.83. Interestingly, the efficiencies of the flexible devices slightly increased when they were bent up or down (up to 25%).

The device efficiencies based on nanotube fibers with different diameters are compared in Table S1 in the Supporting Information. The current densities (J_{sc}) decreased with increasing fiber diameters from 6 to 20 μm, which could be explained as follows: The electrical contact areas between nanotube fibers and electrode were much smaller than the geometric project areas of the nanotube fibers. With increase in the diameter, the geometric project areas of nanotube fibers increased significantly, while the contact areas only slightly increased, so the current densities decreased. To improve the contact area, a nanotube fiber with diameter of 13 μm was replaced with two smaller fibers with the same diameter of 6 μm, and it was found that the J_{sc} value from two smaller fibers increased by about 60% relative to that of the bigger fiber. Also, nanotube fibers were attached to the electrode through van der Waals forces after a series of treatments. However, the relatively small contact areas may limit the stability and efficiency if larger fibers are used to fabricate solar cells. Therefore, the electrical contact area between the fiber and the conductive substrate plays a key role in photocurrent generation. More efforts are underway to understand and optimize the device toward better performance. The V_{oc} values did not change significantly for nanotube fibers with diameters smaller than 10 μm. However, they decreased remarkably with a further increase of diameters above 10 μm, as the charge recombination between electrons and I_3^- ions became more serious with the increasing electron transportation distances, which leads to voltage loss.[31] As a result, the power conversion efficiencies decreased with increasing fiber diameters.

In conclusion, we have developed a novel solar cell from flexible, light-weight, ultrastrong, and semiconductive nanotube fiber. The high alignment of building nanotubes in the fiber allows charges to separate and transport along the fibers efficiently, which provides a fiber solar cell with high performance. The efficiency of the above fiber device may be further improved through the increase of the V_{oc} value by shifting the Fermi level of nanotubes more negatively, increasing FF by improving the electric contact between the fiber and the charge collector, and increasing the J_{sc} value by enhancing the dye loading of the nanotube fiber. This discovery expands the scope of materials and architectures available for high-performance photovoltaic devices.

Received: June 25, 2010
Revised: November 22, 2010
Published online: January 18, 2011

Keywords: carbon · nanotubes · photophysics · solar cells

[1] B. J. Landi, R. P. Raffaelle, S. L. Castro, S. G. Bailey, *Prog. Photovoltaics* **2005**, *13*, 165.
[2] Q. Li, Y. Li, X. Zhang, S. B. Chikkannanavar, Y. Zhao, A. M. Dangelewicz, L. Zheng, S. K. Doorn, Q. Jia, D. E. Peterson, P. N. Arendt, Y. Zhu, *Adv. Mater.* **2007**, *19*, 3358.
[3] C. Yen, Y. Lin, S. Liao, C. Weng, C. Huang, C. Hsieh, C. Ma, M. Chang, H. Shao, M. Tsai, C. Hsieh, C. Tsai, F. Weng, *Nanotechnology* **2008**, *19*, 375305.
[4] S. L. Kim, S. Jang, R. Vittal, J. Lee, K. Kim, *J. Appl. Electrochem.* **2006**, *36*, 1433.
[5] J. E. Trancik, S. C. Barton, J. Hone, *Nano Lett.* **2008**, *8*, 982.
[6] S. Berson, R. de Bettignies, S. Bailly, S. Guillerez, B. Jousselme, *Adv. Funct. Mater.* **2007**, *17*, 3363.
[7] C. Li, Y. Chen, Y. Wang, Z. Iqbal, M. Chhowalla, S. Mitra, *J. Mater. Chem.* **2007**, *17*, 2406.
[8] M. Moniruzzaman, K. I. Winey, *Macromolecules* **2006**, *39*, 5194.
[9] M. Grätzel, *Acc. Chem. Res.* **2009**, *42*, 1788.
[10] M. Schubert, J. H. Werner, *Mater. Today* **2006**, *9*, 42.
[11] H. Qin, S. Wenger, M. Xu, F. Gao, X. Jing, P. Wang, S. M. Zakeeruddin, M. Grätzel, *J. Am. Chem. Soc.* **2008**, *130*, 9202.
[12] J. Liu, M. A. G. Namboothiry, D. L. Carroll, *Appl. Phys. Lett.* **2007**, *90*, 133515.
[13] J. Ramier, C. J. G. Plummer, Y. Leterrier, J. A. E. Manson, B. Echkert, R. Gaudiana, *Renewable Energy* **2008**, *33*, 314.
[14] B. O'Connor, K. P. Pipe, M. Shtein, *Appl. Phys. Lett.* **2008**, *92*, 193306.
[15] X. Fan, Z. Chu, F. Wang, C. Zhang, L. Chen, Y. Tang, D. Zou, *Adv. Mater.* **2008**, *20*, 592.
[16] B. Weintraub, Y. Wei, Z. L. Wang, *Angew. Chem.* **2009**, *121*, 9143; *Angew. Chem. Int. Ed.* **2009**, *48*, 8981.
[17] M. R. Lee, R. D. Eckert, K. Forberick, G. Dennler, C. J. Brabec, R. A. Gaudiana, *Science* **2009**, *324*, 232.
[18] K. Koziol, J. Vilatela, A. Moisala, M. Motta, P. Cunniff, M. Sennett, A. H. Windle, *Science* **2007**, *318*, 1892.
[19] M. Zhang, K. R. Atkinson, R. H. Baughman, *Science* **2004**, *306*, 1358.
[20] K. Jiang, Q. Li, S. Fan, *Nature* **2002**, *419*, 801.

[21] A. B. Dalton, S. Collins E. Muñoz, J. M. Razal, V. H. Ebron, J. P. Ferraris, J. N. Coleman, B. G. Kim, R. H. Baughman, *Nature* **2003**, *423*, 703.
[22] H. Peng, M. Jain, Q. Li, D. E. Peterson, Y. Zhu, Q. Jia, *J. Am. Chem. Soc.* **2008**, *130*, 1130.
[23] H. Peng, J. Menka, D. E. Peterson, Y. Zhu, Q. Jia, *Small* **2008**, *4*, 1964.
[24] H. Peng, X. Sun, F. Cai, X. Chen, Y. Zhu, G. Liao, D. Chen, Q. Li, Y. Lu, Y. Zhu, Q. Jia, *Nat. Nanotechnol.* **2009**, *4*, 738.
[25] H. Ago, T. Kugler, F. Cacialli, W. R. Salaneck, M. S. P. Shaffer, A. H. Windle, R. H. Friend, *J. Phys. Chem. B* **1999**, *103*, 8116–8121.
[26] A. V. Neimark, S. Ruetsch, K. G. Kornev, P. I. Ravikovitch, *Nano Lett.* **2003**, *3*, 419.
[27] C. Perez Leon, L. Kador, B. Peng, M. Thelakkat, *J. Phys. Chem. B* **2006**, *110*, 8723.
[28] B. McCarthy, J. N. Coleman, R. Czerw, A. B. Dalton, M. in het Panhuis, A. Maiti, A. Drury, P. Bernier, J. B. Nagy, B. Lahr, H. J. Byrne, D. L. Carroll, W. J. Blau, *J. Phys. Chem. B* **2002**, *106*, 2210.
[29] M. K. Nazeeruddin, A. Kay, I. Rodicio, R. Humphry-Baker, E. Müller, P. Liska, N. Vlachopoulos, M. Grätzel, *J. Am. Chem. Soc.* **1993**, *115*, 6382.
[30] K. Okazaki, Y. Nakato, K. Murakoshi, *Phys. Rev. B* **2003**, *68*, 035434.
[31] J. Krüger, R. Plass, M. Grätzel, P. J. Cameron, L. M. Peter, *J. Phys. Chem. B* **2003**, *107*, 7536.
[32] L. Qu, L. Dai, M. Stone, Z. Xia, Z. Wang, *Science* **2008**, *322*, 238.

